Synthesis of Tungsten Oxide Nanowires via Thermal Vapor Transport

Benjamin Nail
Chemistry

Faculty Mentor: Shannon Boettcher
Chemistry, Materials Science Institute

Graduate Student Mentor: Adam Smith
Chemistry

Introduction

Tungsten trioxide (WO_3) is an n-type semiconductor that absorbs visible light and has applications in many technologies including gas sensors,[1] electrochromic displays,[9] and devices for photoelectrochemical (PEC) energy conversion.[3] Because of its capacity to absorb visible light, produce photocurrent,[8,6] remain stable in aqueous electrolyte solution,[10] and resist photocorrosion,[4,2] WO_3 may also be used as a photocatalyst for solar water splitting.

Previous researchers have shown that the particle size of a photocatalyst plays a critical role in catalytic ability. Consequently, nanostructured WO_3 has attracted a great deal of research interest in recent years.[6] Tungsten oxide nanowires (NWs) have previously been fabricated by a variety of methods including chemical vapor deposition (CVD), physical vapor deposition (PVD), sol-gel synthesis, and reactive sputtering.[11] The most commonly used method, PVD, involves a WO_3 source material that is

energetically evaporated (sublimed) by heat, ion-bombardment, electron beam, or some other high energy source and then condensed onto targeted substrates. The chemical composition, morphology, and orientation of the resulting PVD grown NWs are significantly affected by the growth conditions such as temperature, substrate material, and the presence of reactive gases.[11]

In spite of the variety of methods reported for the fabrication of 1D crystalline tungsten oxide NWs, the lack of detailed knowledge regarding how specific growth parameters affect nanostructure morphology, com-

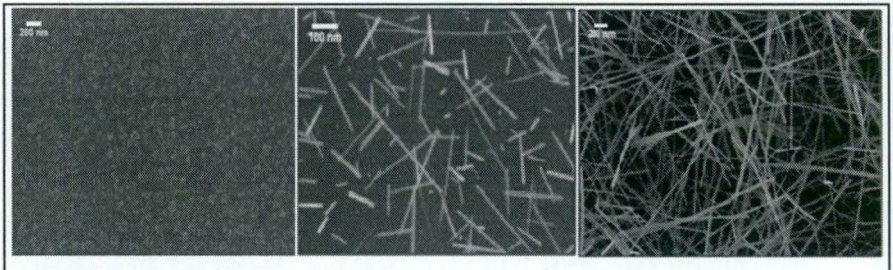

Figure 1. SEM images of WO_2 nanostructures deposited in (**A**) Ar-O_2, (**B**) Ar, and (**C**) Ar-H_2O.

position, and orientation remains an obstacle to the facile synthesis, controllable growth, and further study of these materials. This study examines the effects of O_2 partial pressure and presence of H_2O on the growth of crystalline tungsten oxide NWs.

Experimental Method

Researchers in this study performed all synthesis reactions using a horizontal tube furnace equipped with a quartz working tube (figure 2). All the reagents were analytical grade and used without further purification. Silicon substrates were first subjected to ultrasonic cleaning in commercial solution for 45 min. before being cleaned in a 1:3 mixture of H_2O_2 (30%) : H_2SO_4 (12M) for 15 min. Finally, the substrates were rinsed with

nanopure water and dried in a stream of N_2 gas. A layer of tungsten was deposited on the cleaned substrates by magnetron DC sputtering at 100 W for 100 seconds. Then the substrates were loaded into the low-temperature zone of the tube furnace for the deposition of tungsten oxide vapor.

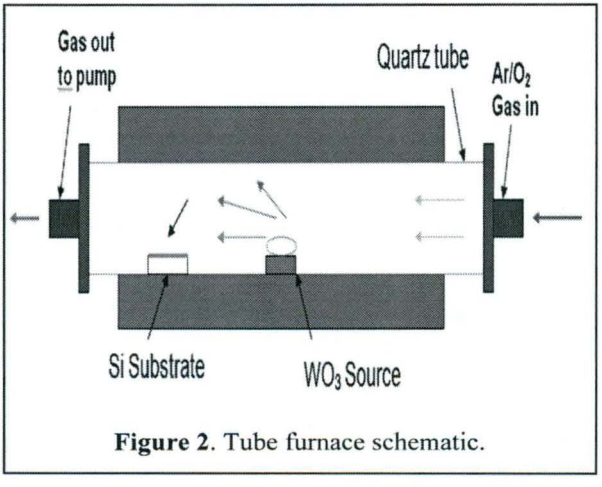

Figure 2. Tube furnace schematic.

The source material, WO_3 powder (Sigma Aldrich; particle size, 12 μm; purity, 99.99%), was placed into a ceramic alumina boat and positioned upstream of the prepared substrates in the high temperature zone of the tube furnace. In some experiments water vapor was introduced by

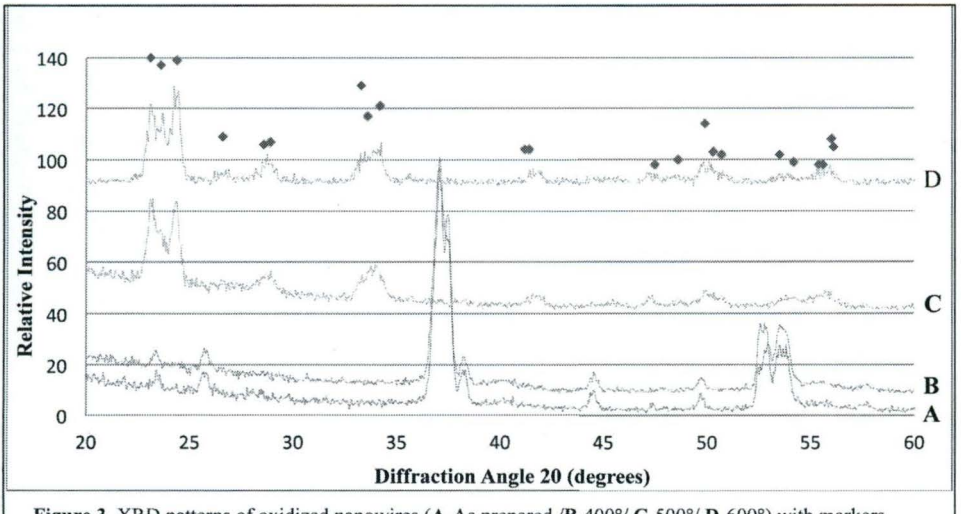

Figure 3. XRD patterns of oxidized nanowires (**A**-As prepared /**B**-400°/ **C**-500°/ **D**-600°) with markers showing known referenced peaks of monoclinic WO_3.

placing an alumina boat filled with 3mL of nanopure H_2O upstream of the source boat in a cool region (<100°C) of the tube furnace. After the quartz tube furnace was reduced to a pressure of approximately 1x10-4 Torr, Ar and O_2 gases were dispensed into the system at the desired rate and ratio using two mass flow controllers (MKS 10 SCCM) that were operated using Labview software, and the system pressure was monitored with a capacitance monometer.

The pressure was maintained at $1x10^{-4}$ Torr ($1\text{-}2x10^{-1}$ Torr for H_2O runs) while the high-temperature region of the tube furnace was increased from room temperature to 700°C at a ramping rate of 25°C/min. After maintaining this temperature for 1 hour, the furnace was allowed to cool naturally to <300°C before removing the samples for characterization.

In the same low-pressure tube furnace, the samples were subjected to a post-synthesis oxidation treatment. First, all materials were removed from the system and the samples were placed in the 700°C region of the furnace. Second, the system pressure was reduced to $1x10^{-4}$ Torr to evacuate any atmospheric gases before dispensing high-purity O_2 gas into the furnace for 15 min. to backfill the furnace tube. Finally the furnace (figure 2) was heated to the desired temperature and maintained at these conditions for 75 min.

The morphology of the deposited nanostructures was observed using a scanning electron microscope (Zeiss Ultra 55) and the crystal structures were analyzed with X-ray diffraction analysis (Philips Panalytical XRD).

Results and Discussion

Figure 1 shows high magnification SEM images of the Si substrates after the vapor deposition procedure. All three samples were deposited at 685°C for 75 min. at a pressure of 200mTorr. The sample synthesized in the presence of O_2 gas (sample A) shows tungsten oxide deposition only

in the form of platelets with no NW growth. Because the amount of O_2 gas present during the synthesis of this sample was only 5% of the total gas mixture, the lowest output our equipment could achieve, we hypothesize that even a small quantity of O_2 gas will react with vapor from the WO_3 powder to form an oxygen rich species (not WO_2) that lacks the ability to form 1D NWs. In contrast, the sample synthesized in inert gas (sample B) displayed some sparse growth of NWs, suggesting that a more oxygen deficient vapor species WO_{3-x} lends itself to the formation of 1D NWs. Sample C was formed in the presence of H_2O vapor and the resulting SEM images show densely grown NWs with lengths of hundreds of nanometers (figure 4).

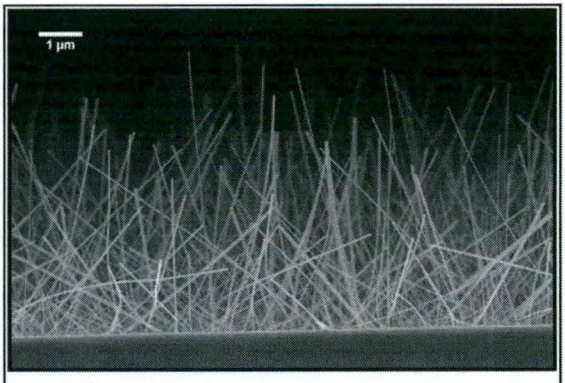

Figure 4. Cross sectional SEM image of sample C.

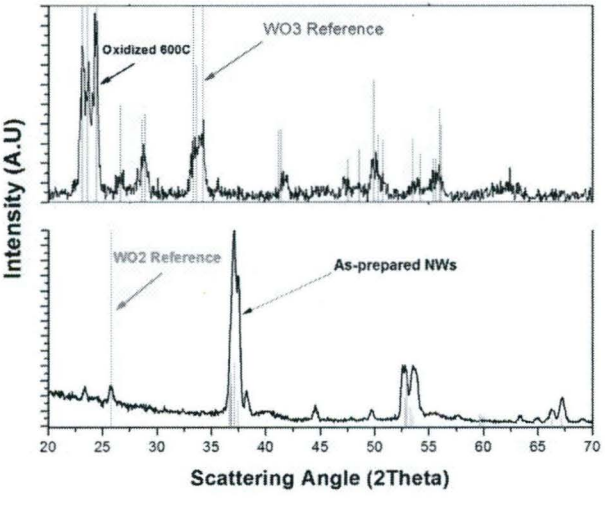

Figure 5. XRD spectra of NWs before (bottom) and after (top) 600° C Oxidation with vertical reference peaks.

To explain the considerable

increase in the growth density and length of the NWs produced in sample C, we propose a mechanism by which the added H_2O vapor reacts with WO_3 to form the far more volatile hydrate species $WO_3 \cdot H_2O$. That hydrate, under conditions of high heat and humidity, is known to have a much higher volatility than any other tungsten oxide species present in our system.[10] Since a species with higher volatility will enter the vapor phase more readily than one with lower volatility, the hydrate may assist in the effective vapor transport processes, from source to substrate, by allowing more tungsten containing species into the vapor phase at any given time. Ensuring a steady and sufficient flow of tungsten oxide vapor to the growth sites by introducing H_2O into the system may explain the profound increase in both the length and abundance of the NWs in sample C.

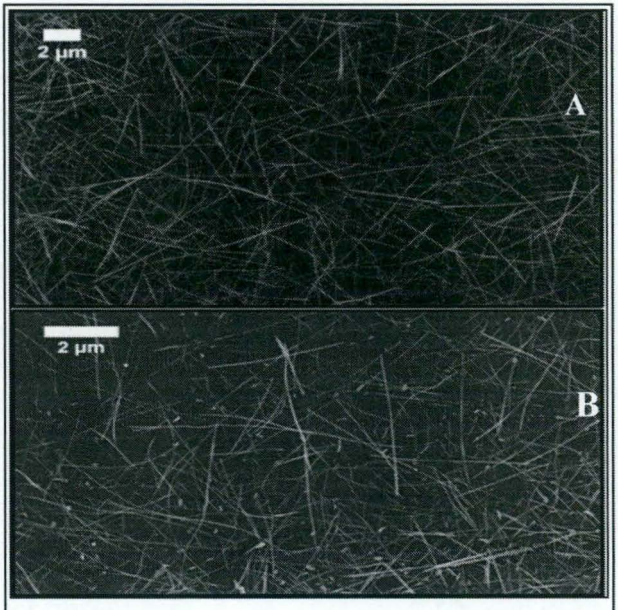

Figure 6. *SEM images of NWs as-prepared (A) and after 600°C Oxidation (B)*

The XRD patterns in figure 3 illustrate the controlled transformation of the as-synthesized WO_2 NWs (bottom) to monoclinic WO_3 NWs (top) during the low-pressure oxidation procedure. For the as-prepared XRD

patterns (bottom), we indexed the peaks at 25.8°, 36.4°, 53.4°, and 67.1° to the structure of WO_2. For the top pattern we indexed the primary peaks at 23.1°, 23.5°, 24.4°, 26°, 29.2°, 33.2°, 34.1°, and several others to the structure of monoclinic WO_3. Figure 5 shows the XRD patterns of the as-synthesized NWs and the fully oxidized NWs superimposed with referenced peak positions.

Contrary to some reports in the literature regarding the degradation of WO_x NWs during high temperature oxidation, the NWs oxidized in this study, oxidized between 400°-600°C, were completely intact (figure 6). We believe the low-pressure oxidation conditions used in our procedure may have played a crucial role in retaining the 1D morphology during oxidation.

Conclusion

In summary, our research group has synthesized WO_2 NWs on W sputtered Si substrates by physical vapor deposition in the presence of H_2O vapor and controllably oxidized the as-synthesized WO_2 NWs to monoclinic WO_3 by a high-oxygen low-pressure annealing treatment. The densely grown NWs were 10-60 nm in diameter and 1-3 μm in length. We found that the choice of gas mixture in the growth environment played a critical role in the density and morphology of the NWs. Additionally, we propose a vapor-solid (VS) growth mechanism for the NW growth in this study due to the fact that no liquid phase catalyst was present during the reaction.

The XRD study confirmed that the as-synthesized NWs were not of the desired stoichiometric composition (WO_3) but could be transformed from WO_2 to WO_3 through a post-synthesis annealing treatment under vacuum in a high O_2 environment. In contrast to some reports in the literature, we were able to observe the preferred 1D NW morphology even after our

annealing treatment. Further study on this topic would benefit from a more controlled method of introducing H_2O vapor so that the effect of relative humidity on NW synthesis can be better understood. Future plans for our research in this area include transmission electron microscope (TEM) studies of the NW crystal structure, electron beam induced current (EBIC) analysis, and electrochemical analysis of NW electrodes to evaluate their catalytic ability as a possible photoelectrocatalyst.

A particularly promising application of WO_3 NWs that should be considered is their function as a photoanode material in photoelectrochemical cells for solar energy conversion and storage purposes.

Acknowledgements

This research was supported by the University of Oregon McNair Scholars Program and the University of Oregon Department of Chemistry. The author would like to thank the Camcor Materials Characterization facilities at the University of Oregon as well as the following individuals for their assistance with this work; Paul Plassmeyer, Lena Trotochaud, Ngoc Nguyen, Kurt Langworthy, Andy Ritenour, and the great elusive nanowire.

References

1. Smith, D. J.; Vatelino, J. F.; Falconer, R. S.; Wittman, E. L. Stability, Sensitivity and Selectivity of Tungsten Trioxide Films for Sensing Applications. *Sens. Actuators* B 1993, 13, 264-268.

2. Scaife, D. E. Oxide Semiconductors in Photoelectrochemical Conversion of Solar Energy. *Solar Energy* 1980, 25, 41-54.

3. Butler, M. A. Photoelectrolysis and Physical Properties of the Semiconducting Electrode WO_2. *J. Appl. Phys.* 1977, 48 1914-1920.

4. Butler, M. A.; Nasby, R. D.; Quinn, R. K. Tungsten Trioxide as an Electrode for Photoelectrolysis of Water. *Solid State Comm.* 1976, 19, 1011-1014.

5. Miller, E. L.; Rocheleau, R. E.; Deng, X. M. Design Considerations for a Hybrid Amorphous Silicon/Photoelectrochemical Multijunction Cell for Hydrogen Production. *Int. J. Hydrogen Energy* 2003, 28, 615-623.

6. Santato, C.; Ulmann, M.; Augustynski, J. Photoelectrochemical Properties of Nanostructured Tungsten Trioxide Films. *J. Phys. Chem. B* 2001,105, 936-940.

7. Berak, J. M.; Sienko, M. J. Effect of Oxygen-deficiency on Electrical Transport Properties of Tungsten Trioxide Crystals. *J. Solid State Chem.* 1970, 2, 109-133.

8. Hodes, G., Cahen, D., Manassen, J. Tungsten Trioxide as a Photoanode for a Photoelectrochemical Cell (PEC). *Nature* 1976, 260, 312-313.

9. Granqvist, C. G. Electrochromic Tungsten Oxide Films: Review of Progress 1993–1998. *Sol. Energy Mater. Sol. C*ells 2000, 60, 201-262.

10. Lassner, E.; Schubert, W. *Tungsten: Properties, Chemistry, Technology of the Element, Alloys, and Chemical Compounds*; Kluwer Academic: New York, 1999.

11. Zheng, H., Ou, J. Z., Strano, M. S., Kaner, R. B., Mitchell, A., Kalantar-zadeh, K. Nanostructured Tungsten Oxide – Properties, Synthesis, and Applications. *Adv. Funct. Mater.* 2011, 21, 2175–2196.